Reexamination of the role of the Δ^* resonances in the $pp \to nK^+\Sigma^+$ reaction

Xiao-Yun Wang,[1,2,3,*] Xu Cao,[1,3,4,†] Ju-Jun Xie,[1,3,4,‡] and Xu-Rong Chen[1,3]

[1]*Institute of Modern Physics, Chinese Academy of Sciences, Lanzhou 730000, China*

[2]*University of Chinese Academy of Sciences, Beijing 100049, China*

[3]*Research Center for Hadron and CSR Physics, Institute of Modern Physics of CAS and Lanzhou University, Lanzhou 730000, China*

[4]*State Key Laboratory of Theoretical Physics, Institute of Theoretical Physics, Chinese Academy of Sciences, Beijing 100190, China*

(Received 21 December 2014; revised manuscript received 3 June 2015; published 8 July 2015)

In this work, the role of the Δ^* resonances in the process of $pp \to nK^+\Sigma^+$ are systematically investigated with the effective Lagrangian approach and the isobar model. We find that a P_{31} state, either $\Delta^*(1750)$ or $\Delta^*(1910)$ is favored by the data while the P_{33} state, namely $\Delta^*(1920)$, has small contribution. Besides, either the subthreshold S_{31} $\Delta^*(1620)$ resonance or strong $n\Sigma$ final state interaction or both have a possible contribution at near threshold region, depending on the measured cross sections. We demonstrate the invariant mass distributions and the Dalitz plots in order to investigate whether it is possible to distinguish the controversial $K\Sigma$ production mechanism in these observables.

DOI: 10.1103/PhysRevC.92.015202   PACS number(s): 14.20.Gk, 13.75.Cs, 13.30.Eg

I. INTRODUCTION

The baryon spectrum has attracted a lot of theoretical and experimental interest for a long time because it is expected to reveal important information on the internal structure of baryons and the mechanism of quark confinement. The phenomenological models [1–4] predict the excited states of N^* and Δ^*, and recently lattice QCD has been used to calculated the spectrum in finite volume [5,6]. However, although some of the predicted states have been identified from the πN and γN scattering data, many of them have not yet been observed in any experiments [7–10]. These states, so called as the *missing resonances*, are for what we are searching [11]. Therefore, it is necessary and meaningful to search for these states and study their properties in other reactions.

The $pp \to nK^+\Sigma^+$ reaction is a very ideal channel for studying the Δ^* resonances with isospin 3/2 since the contributions of the N^* with isospin 1/2 are filtered out in this channel. Some results have been obtained on the experimental and theoretical aspects, however, they are far from being sufficient to reveal the contribution of the Δ^* on the basis of these results.

At present, there are only a few experimental data on the total cross section of the $pp \to nK^+\Sigma^+$ reaction [12–17]. What is worse, it is known that the close-to-threshold data are inconsistent between the COSY-11, HIRES, and COSY-ANKE groups. The total cross section data from COSY-11 shows strong close-threshold enhancement [13], however, not confirmed by the measurement of other two groups. The COSY-ANKE data follow the behavior of three-body phase-space [14,15] and the values are about one order smaller than that of the COSY-11 at the same energy range [13]. Moreover, the HIRES data [16] at beam energy $T_p = 2.08$ GeV make the situation more complex and its value is around three times bigger than the COSY-ANKE data at $T_p = 2.16$ GeV [14]. Valdau and Wilkin argued that the HIRES data determined from the inclusive K^+-meson production in pp collisions should be considered as an upper bound so it does not conflict with the result of COSY-ANKE [17].

On the theoretical side, most of the previous studies focus on the contribution of the $\Delta^*(1920)$ and $\Delta^*(1620)$ resonances in the $pp \to nK^+\Sigma^+$ reaction. Tsushima *et al.* introduced the effective intermediate $\Delta^*(1920)$ resonance to account for the contribution of several Δ^* state around 1900 MeV [18–22] and their calculations reproduced the experiment data at high energies very well. However, the coupling of $\Delta^*(1920)$ to the $K\Sigma$ in relative P wave is suppressed at close-to-threshold energies. In order to explain the large near-threshold data of COSY-11, Xie *et al.* [23] suggested the $\Delta^*(1620)$ resonance below the $K\Sigma$ threshold as the possible source of the very strong near-threshold enhancement. Later, Cao *et al.* [24] further pointed out that an unusually strong $n\Sigma$ final state interaction was needed to fully interpret the COSY-11 data. In these calculations, the coupling constant of the $\Delta^*(1620)$ to $K\Sigma$ determined by the relation $g_{\Delta^*(1620)\Sigma K} = g_{\Delta^*(1620)\pi N}$ from the SU(3) symmetry has a big uncertainty because the mass of $\Delta^*(1620)$ is below the $K\Sigma$ threshold.

The above situation indicates that the production mechanism of the $pp \to nK^+\Sigma^+$ reaction is still an open question. As a matter of fact, there is a long discrepancy of various coupled-channel studies of the $\pi^+p \to K^+\Sigma^+$ reaction, where only the Δ^* resonances are allowed, the same as the $pp \to nK^+\Sigma^+$ channel. The Juelich model [25–28] finds that the $\Delta^*(1620)$ is dominant in the low energies of this reaction, while the Bonn-Gatchina partial wave analysis identifies the $\Delta^*(1920)$ as the most essential contribution [29,30]. The Giessen model with the K-matrix approximation claims the vital role of the $\Delta^*(1750)$ at close-threshold range [31–34]. The confusion is not relieved [29,32,34] in the $\pi^-p \to K\Sigma$ and $\gamma N \to K\Sigma$ reactions where the N^* resonances are also contributing, though more data are available there. The situation at high energies is even more complicated and several partial waves are important.

*xywang@impcas.ac.cn

†Corresponding author: caoxu@impcas.ac.cn

‡xiejujun@impcas.ac.cn

In this work, we systematically study the role of Δ^{*++} resonances in the $pp \to nK^+\Sigma^+$ channel in order to properly clarify the present confusion and shed light on the future measurements. This paper is organized as follows. After the Introduction, we illustrate our investigative method and formalism. In Sec. III, the numerical results are presented and discussed. We propose two possible schemes to interpret the contribution of Δ^{*++} resonances in the $pp \to nK^+\Sigma^+$ reaction. Finally, a short summary is given in Sec. IV.

II. METHOD AND FORMALISM

In the present work, we use the effective Lagrangian approach and the isobar model in terms of hadrons to study the process of $pp \to nK^+\Sigma^+$ and $\pi^+p \to K^+\Sigma^+$, where the $K^+\Sigma^+$ are produced through the intermediate $\Delta^*(1620)$, $\Delta^*(1750)$, $\Delta^*(1910)$, and $\Delta^*(1920)$ resonances. Besides, the π-meson exchange in the pp collisions is considered in the proton-proton collisions. Another meson, e.g., the ρ-meson exchange, is not included and this is not unanimous in the modeling of the $pp \to nK^+\Sigma^+$ reaction within a meson-exchange picture. Fortunately, the estimation of the $pp \to nK^+\Sigma^+$ cross section in our model is sensitive to the couplings of different Δ^* resonances to the $K\Sigma$ channel, which are determined from the $\pi^+p \to K^+\Sigma^+$ reaction. Hence, the single-pion exchange is enough for this purpose. By neglecting the ρ-meson exchange, we can give a unified picture of pion- and proton-induced reactions, though our theoretical results are more general than this would suggest.

At present it is still under debate which P_{31} state, the $\Delta^*(1750)$ or $\Delta^*(1910)$ resonance, has a strong coupling to $K\Sigma$, as discussed in Sec. I. Based on the limited data of the $pp \to nK^+\Sigma^+$ reaction, it is impossible to unambiguously pin down the relevant masses at this stage. So herein we include these two P_{31} states separately, leading to two solutions with different amplitudes,

$$\mathcal{M}_I = \mathcal{M}_{\Delta^*(1620)} + \mathcal{M}_{\Delta^*(1910)} + \mathcal{M}_{\Delta^*(1920)}, \quad (1)$$

$$\mathcal{M}_{II} = \mathcal{M}_{\Delta^*(1620)} + \mathcal{M}_{\Delta^*(1750)} + \mathcal{M}_{\Delta^*(1920)} \quad (2)$$

as summarized in Table I. This is also in line with the study of the $\pi^+p \to K^+\Sigma^+$ reaction in different models [25–34], which usually include only one of the P_{31} states. Correspondingly we will consider these two solutions in the $\pi^+p \to K^+\Sigma^+$ reaction in the following calculation.

A. Feynman diagrams and effective Lagrangian

The basic tree-level Feynman diagrams for the $pp \to nK^+\Sigma^+$ reaction are presented in Fig. 1, and the s-channel diagram for the $\pi^+p \to K^+\Sigma^+$ reaction is depicted in Fig. 2. The t-channel diagram for the $\pi^+p \to K^+\Sigma^+$ reaction is calculated as being small [34]. This is reasonable because the exchanged K and K^* mesons in the t-channel have a small coupling to the relevant $N\Sigma$ and πK channels. The interference of the u and t channels with s-channel resonances contribution are important for describing the differential and polarization observables [34], but it is safe to ignore them in the determination of the coupling constants of the dominant resonances in the s channel.

TABLE I. The considered Δ^* resonances in the model.

Resonances	Width (MeV)	J^P	Solution I	Solution II
$\Delta^*(1620)S_{31}$	140	$1/2^-$	√	√
$\Delta^*(1750)P_{31}$	300	$1/2^+$	—	√
$\Delta^*(1910)P_{31}$	250	$1/2^+$	√	—
$\Delta^*(1920)P_{33}$	220	$3/2^+$	√	√

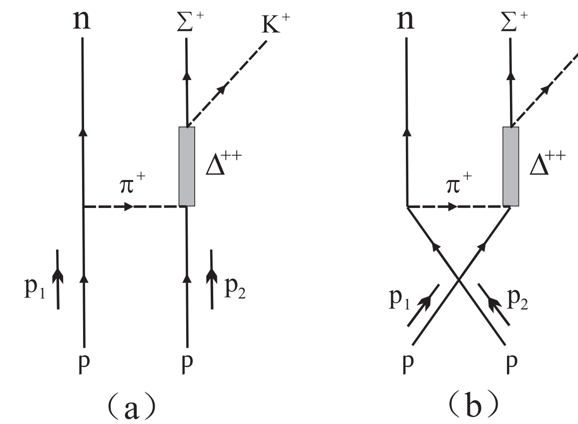

FIG. 1. Feynman diagram for the $pp \to nK^+\Sigma^+$ reaction.

For the interaction vertex of πNN, we use the effective pseudoscalar coupling [18–20]

$$\mathcal{L}_{\pi NN} = -ig_{\pi NN}\bar{N}\gamma_5\vec{\tau}\cdot\vec{\pi}N. \quad (3)$$

The Lagrangians of $\Delta^*N\pi$ and $\Delta^*K\Sigma$ vertices are used by many models, such as the Jülich model, Giessen model, and Bonn-Gatchina model [27,29,31]. But the elementary Lorentz structure which depends on the relative orbital momentum and spin are the same. Therefore, the general effective Lagrangian for the vertices of $\Delta^*N\pi$ and $\Delta^*\Sigma K$ read as follows:

$$\mathcal{L}_{\Delta^*(1620)N\pi} = \frac{g_{\Delta^*(1620)N\pi}}{m_\pi}\bar{\Delta}^*\gamma^\mu\vec{\tau}\cdot\partial_\mu\vec{\pi}N + \text{H.c.}, \quad (4)$$

$$\mathcal{L}_{\Delta^*(1620)\Sigma K} = \frac{g_{\Delta^*(1620)\Sigma K}}{m_K}\bar{\Delta}^*\gamma^\mu\vec{\tau}\cdot\partial_\mu\vec{K}\Sigma + \text{H.c.}, \quad (5)$$

$$\mathcal{L}_{\Delta^*(1750)N\pi} = -\frac{g_{\Delta^*(1750)N\pi}}{m_{\Delta^*(1750)}}\bar{\Delta}^*\gamma_5\gamma_\mu\vec{\tau}\cdot\partial^\mu\vec{\pi}N + \text{H.c.}, \quad (6)$$

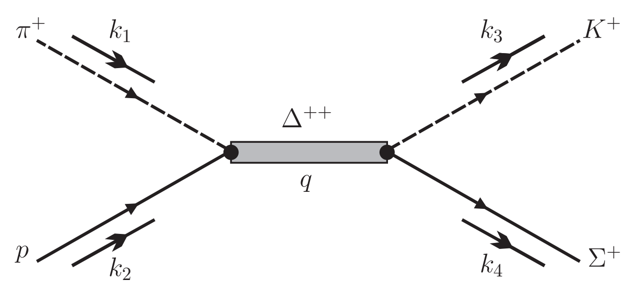

FIG. 2. Feynman diagram for the $\pi^+p \to K^+\Sigma^+$ reaction.

$$\mathcal{L}_{\Delta^*(1750)\Sigma K} = -\frac{g_{\Delta^*(1750)\Sigma K}}{m_{\Delta^*(1750)}}\bar{\Delta}^*\gamma_5\gamma_\mu\vec{\tau}\cdot\partial^\mu\vec{K}\Sigma + \text{H.c.}, \quad (7)$$

$$\mathcal{L}_{\Delta^*(1910)N\pi} = -\frac{g_{\Delta^*(1910)N\pi}}{m_{\Delta^*(1910)}}\bar{\Delta}^*\gamma_5\gamma_\mu\vec{\tau}\cdot\partial^\mu\vec{\pi}N + \text{H.c.}, \quad (8)$$

$$\mathcal{L}_{\Delta^*(1910)\Sigma K} = -\frac{g_{\Delta^*(1910)\Sigma K}}{m_{\Delta^*(1910)}}\bar{\Delta}^*\gamma_5\gamma_\mu\vec{\tau}\cdot\partial^\mu\vec{K}\Sigma + \text{H.c.}, \quad (9)$$

$$\mathcal{L}_{\Delta^*(1920)N\pi} = -\frac{g_{\Delta^*(1920)N\pi}}{m_{\Delta^*(1920)}}\bar{\Delta}^*_\mu\vec{\tau}\cdot\partial^\mu\vec{\pi}N + \text{H.c.}, \quad (10)$$

$$\mathcal{L}_{\Delta^*(1920)\Sigma K} = -\frac{g_{\Delta^*(1920)\Sigma K}}{m_{\Delta^*(1920)}}\bar{\Delta}^*_\mu\vec{\tau}\cdot\partial^\mu\vec{K}\Sigma + \text{H.c.}, \quad (11)$$

where $\vec{\tau}$ is the Pauli matrix, and Δ^* and Δ^*_μ stand for the fields of the corresponding baryon resonances.

B. Propagator and form factor

The propagator of the π meson is

$$G_\pi(q_\pi) = \frac{-i}{q_\pi^2 - m_\pi^2}. \quad (12)$$

The propagators for the resonance Δ^* can be constructed through the projection operator and Breit-Wigner factor [35]. For the $\Delta^*(1620)$, $\Delta^*(1750)$, and $\Delta^*(1910)$ with spin-1/2, the propagator can be written as

$$G^{\frac{1}{2}}_{\Delta^*}(q_{\Delta^*}) = -i\frac{\not{q}_{\Delta^*} + m_{\Delta^*}}{q_{\Delta^*}^2 - m_{\Delta^*}^2 + i m_{\Delta^*}\Gamma_{\Delta^*}}. \quad (13)$$

For $\Delta^*(1920)$ with spin-3/2, we have

$$G^{3/2}_{\Delta^*}(q_{\Delta^*}) = G^{1/2}_{\Delta^*}(q_{\Delta^*})G_{\mu\nu}(q_{\Delta^*}), \quad (14)$$

$$G^{\mu\nu}_{\Delta^*}(q_{\Delta^*}) = -i\frac{\not{q}_{\Delta^*} + m_{\Delta^*}}{q_{\Delta^*}^2 - m_{\Delta^*}^2 + i m_{\Delta^*}\Gamma_{\Delta^*}} \times\left[g^{\mu\nu} - \frac{1}{3}\gamma^\mu\gamma^\nu - \frac{(\gamma^\mu q^\nu_{\Delta^*} - \gamma^\nu q^\mu_{\Delta^*})}{3m_{\Delta^*}} - \frac{2q^\mu_{\Delta^*}q^\nu_{\Delta^*}}{3m^2_{\Delta^*}}\right]. \quad (15)$$

At each vertex a relevant off-shell form factor is used to suppress the contributions from high exchanged momenta. In our computation, we take the same form factors as those used in the well-known Bonn model for the πNN and $\Delta^* N\pi$ vertices [36]

$$F^{NN}_\pi(q_\pi^2) = \frac{\Lambda_\pi^2 - m_\pi^2}{\Lambda_\pi^2 - q_\pi^2} \quad (16)$$

$$F^{\Delta^* N}_\pi(q_\pi^2) = \frac{\Lambda_\pi^{*2} - m_\pi^2}{\Lambda_\pi^{*2} - q_\pi^2}, \quad (17)$$

where q_π and $\Lambda_\pi^{(*)}$ are the four-momentum and cut-off parameters for the exchange π meson, respectively. We take $\Lambda_\pi = 0.8$ GeV for all resonances and $\Lambda^*_\pi = 0.8$ GeV, 1.0 GeV, 1.2 GeV, and 1.2 GeV for the $\Delta^*(1620)$, $\Delta^*(1750)$, $\Delta^*(1910)$, and $\Delta^*(1920)$ resonances, respectively. They are determined by the data of $pp \to nK^+\Sigma^+$. The Λ^*_π of $\Delta^*(1620)$ can be determined in the close-to-threshold region while those of the $\Delta^*(1750)$ and $\Delta^*(1910)$ can be pinned down at higher energies. The uncertainty of the Λ^*_π for $\Delta^*(1920)$ is relatively bigger because its contribution is small. For consistency, we set it to be the same as that of $\Delta^*(1910)$.

Besides, the form factor for the off-shell resonances is taken as

$$F_{\Delta^*}(q^2_{\Delta^*}) = \frac{\Lambda^4_{\Delta^*}}{\Lambda^4_{\Delta^*} + (q^2 - m^2_{\Delta^*})^2}, \quad (18)$$

which is used to depict the resonances in the $\pi^+ p \to K^+\Sigma^+$ and $pp \to nK^+\Sigma^+$ reactions. The revelent cut-off parameters $\Lambda_{\Delta^*} = 1.7$ GeV are taken to be around the mass of resonances in both reactions and the calculated results are not very sensitive to this value.

C. Coupling constants

The coupling constant of the πNN interaction was given in many theoretical works, and we take $g^2_{\pi NN}/4\pi = 12.96$ [37,38]. According to the above Lagrangians, the partial decay widths which are related to the coupling constants can be written as follows:

$$\Gamma_{\Delta^*(1620)\to N\pi} = \frac{g^2_{\Delta^*(1620)N\pi}(E_N + m_N)|\vec{p}_N^{\,\text{c.m.}}|}{4\pi m_{\Delta^*(1620)}m_\pi^2} \times (m_{\Delta^*(1620)} - m_N)^2, \quad (19)$$

$$\Gamma_{\Delta^*(1750)\to N\pi} = \frac{g^2_{\Delta^*(1750)N\pi}(E_N - m_N)|\vec{p}_N^{\,\text{c.m.}}|}{4\pi m^3_{\Delta^*(1750)}} \times (m_{\Delta^*(1750)} + m_N)^2, \quad (20)$$

$$\Gamma_{\Delta^*(1910)\to N\pi} = \frac{g^2_{\Delta^*(1910)N\pi}(E_N - m_N)|\vec{p}_N^{\,\text{c.m.}}|}{4\pi m^3_{\Delta^*(1910)}} \times (m_{\Delta^*(1910)} + m_N)^2, \quad (21)$$

$$\Gamma_{\Delta^*(1920)\to N\pi} = \frac{g^2_{\Delta^*(1920)N\pi}(E_N + m_N)}{12\pi m^3_{\Delta^*(1920)}}|\vec{p}_N^{\,\text{c.m.}}|^3, \quad (22)$$

where the E_N, E_π, and $\vec{p}_N^{\,\text{c.m.}}$ are defined in the center of mass (c.m.) system:

$$E_N = \frac{M^2_{\Delta^*} + m^2_N - m^2_\pi}{2M_{\Delta^*}},$$

$$|\vec{p}_N^{\,\text{c.m.}}| = \sqrt{E_N^2 - m_N^2}.$$

For the $\Delta^* \to K\Sigma$ decays, the formulas are basically identical to those for $\Delta^* \to \pi N$ with the replacement of π and N to K and Σ, respectively. With the experimental masses, total decay widths, and branching ratios [39], we can obtain all relevant Δ^* resonance parameters from above formulas as summarized in Table II. In this table, all the known branching ratios of the $\Delta^*(1620)$, $\Delta^*(1750)$, $\Delta^*(1910)$, and $\Delta^*(1920)$ resonances are taken from the Particle Data Group (PDG) [39].

Since the mass of the $\Delta^*(1620)$ is below the threshold of the $K\Sigma$, the coupling of the $\Delta^*(1620)$ to $K\Sigma$ cannot be determined by the corresponding decay width. Also,

TABLE II. Relevant parameters for Δ^* resonances. The values labeled with a dagger "†" are extracted from the data of $\pi^+ p \to K^+\Sigma^+$ reaction and others are from the compilation of PDG [39].

Resonances	mass (MeV)	width (MeV)	channel	Branching ratio (%)	$g^2/4\pi$
$\Delta^*(1620)$	1615	140	πN	25.0	0.002
			$K\Sigma$	–	$0.053^\dagger$
$\Delta^*(1750)$	1750	300	πN	10.0	0.20
			$K\Sigma$	7.1	$2.96^\dagger$
$\Delta^*(1910)$	1875	250	πN	22.5	0.288
			$K\Sigma$	14.0	0.953
$\Delta^*(1920)$	1910	220	πN	12.5	0.730
			$K\Sigma$	2.14	0.510

there is no so much information on the coupling strength of the $\Delta^*(1750)K\Sigma$ vertex. In our calculation, they are treated as free parameters and fitted to the data of the $\pi^+ p \to K^+\Sigma^+$ reaction. Following the Feynman rules and using the above Lagrangian, the theoretical invariant amplitude $\mathcal{A}$ of $\pi^+ p \to K^+\Sigma^+$ reaction in Fig. 2 could be calculated as

$$\begin{aligned}\mathcal{A}_I = & \frac{g_{\Delta^*(1620)N\pi}\, g_{\Delta^*(1620)\Sigma K}\, F_{\Delta^*(1620)}(q^2_{\Delta^*})}{m_K m_\pi} \\ & \times \bar{u}(k_4)\, \not{k}_3 G_{\Delta^*(1750)}(q^2_{\Delta^*})\, \not{k}_1 u(k_2) \\ & + \frac{g_{\Delta^*(1750)N\pi}\, g_{\Delta^*(1750)\Sigma K}\, F_{\Delta^*(1750)}(q^2_{\Delta^*})}{m^2_{\Delta^*(1750)}} \\ & \times \bar{u}(k_4)\gamma_5\, \not{k}_3 G_{\Delta^*(1750)}(q^2_{\Delta^*})\, \not{k}_1 \gamma_5 u(k_2) \\ & + \frac{g_{\Delta^*(1920)N\pi}\, g_{\Delta^*(1920)\Sigma K}\, F_{\Delta^*(1920)}(q^2_{\Delta^*})}{m^2_{\Delta^*(1920)}} \\ & \times \bar{u}(k_4) k_{3\mu} G^{\mu\nu}_{\Delta^*(1920)}(q^2_{\Delta^*}) k_{1\nu} u(k_2) \quad , \end{aligned} \tag{23}$$

if assuming the intermediate P_{31} excitation is the $\Delta^*(1750)$ resonance. Here the propagator G_{Δ^*} and the form factor F_{Δ^*} of the Δ^* resonance can be found in the following subsection. By integrating the amplitude in the two-body phase space, we can easily obtain the total cross sections of the $\pi^+ p \to K^+\Sigma^+$ reaction as function of the momentum of beam particle π^+ meson. By fitting the coupling constants of $\Delta^*(1620)K\Sigma$ and $\Delta^*(1750)K\Sigma$, we achieve a good agreement ($\chi^2 = 3.6$) between the model and the experimental data, as shown in Fig. 3(a) and Table II. The extracted parameter $g^2_{\Delta^*(1750)\Sigma K}/4\pi = 2.96$ gives a reasonable branch ratio 7.1% of $\Delta^*(1750) \to K\Sigma$, which is around one order larger than that in the refined Giessen model (0.9%) [34]. However, it should be noted that the mass and total width of $\Delta^*(1750)$ are different in two approaches. Our $g^2_{\Delta^*(1620)\Sigma K}/4\pi = 0.053$ is about one order smaller than the value from SU(3) symmetry in Ref. [23], but in the same level with the value of the Giessen model [34]. In an alternative explanation of the $\pi^+ p \to K^+\Sigma^+$ data, the $\Delta^*(1750)$ would be replaced by the $\Delta^*(1910)$ in Eq. (23), corresponding to the amplitudes $\mathcal{A}_{II}$ in solution II ($\chi^2 = 4.6$). The calculated total cross section of $\pi^+ p \to K^+\Sigma^+$ with

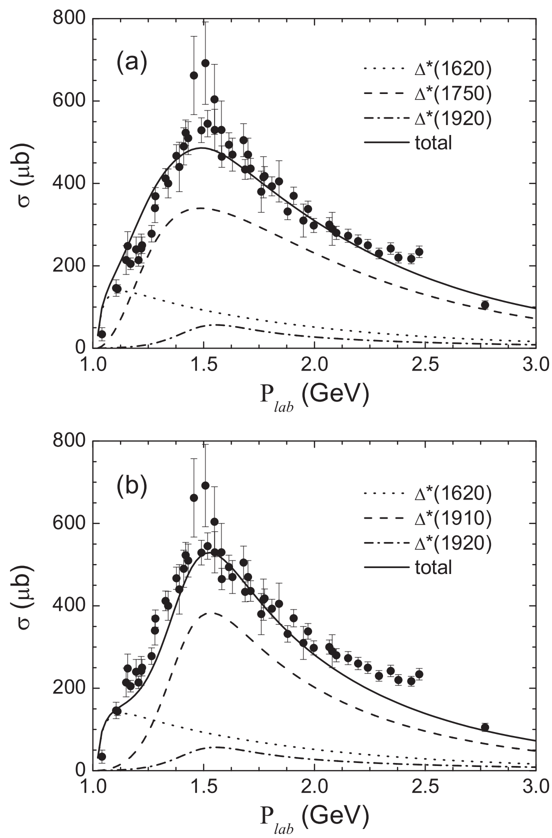

FIG. 3. Total cross section including the contributions of $\Delta^*(1750)$ resonance versus the beam momentum $P_{\rm lab}$ for $\pi^+ p \to K^+\Sigma^+$ reaction. The experimental data are taken from Ref. [12].

the parameters in Table II are shown in Fig. 3(b). As can be seen, the two solutions both give a fair reproduction of the data, reflecting the validity and consistency of our parameters.

D. Amplitude

According to above effective Lagrangian and the Feynman rules, the invariant amplitudes of the $\Delta^*(1620)$, $\Delta^*(1750)$, $\Delta^*(1910)$, and $\Delta^*(1920)$ resonances contribution in the $pp \to nK^+\Sigma^+$ reaction could be read as

$$\begin{aligned}\mathcal{M}_{\Delta^*(1620)} = & \frac{\sqrt{2} g_{\pi NN}\, g_{\Delta^*(1620)\Sigma K}\, g_{\Delta^*(1620)N\pi}}{m_K m_\pi} \\ & \times F^{NN}_\pi(q^2_\pi) F^{\Delta^* N}_\pi(q^2_\pi) F_{\Delta^*}(q^2_{\Delta^*}) \\ & \times \bar{u}_\Sigma(p_\Sigma)\, \not{p}_K G^{\frac{1}{2}}_{\Delta^*}(q_{\Delta^*})\, \not{p}_\pi \\ & \times u_N(p_1) G_\pi(q_\pi) \bar{u}_N(p_n)\gamma_5 u_N(p_2), \end{aligned} \tag{24}$$

$$\begin{aligned}\mathcal{M}_{\Delta^*(1750)} = & \frac{\sqrt{2} g_{\pi NN}\, g_{\Delta^*(1750)N\pi}\, g_{\Delta^*(1750)\Sigma K}}{m^2_{\Delta^*(1750)}} \\ & \times F^{NN}_\pi(q^2_\pi) F^{\Delta^* N}_\pi(q^2_\pi) F_{\Delta^*}(q^2_{\Delta^*}) \\ & \times \bar{u}_\Sigma(p_\Sigma)\gamma_5\, \not{p}_K G^{\frac{1}{2}}_{\Delta^*}(q_{\Delta^*})\, \not{p}_\pi \gamma_5 \\ & \times u_N(p_1) G_\pi(q_\pi) \bar{u}_N(p_n)\gamma_5 u_N(p_2), \end{aligned} \tag{25}$$

$$\mathcal{M}_{\Delta^*(1910)} = \frac{\sqrt{2} g_{\pi NN} g_{\Delta^*(1910)N\pi} g_{\Delta^*(1910)\Sigma K}}{m^2_{\Delta^*}(1910)} \times F_\pi^{NN}(q_\pi^2) F_\pi^{\Delta^* N}(q_\pi^2) F_{\Delta^*}(q_{\Delta^*}^2) \times \bar{u}_\Sigma(p_\Sigma)\gamma_5 \not{p}_K G^{\frac{1}{2}}_{\Delta^*}(q_{\Delta^*}) \not{p}_\pi \gamma_5 \times u_N(p_1) G_\pi(q_\pi) \bar{u}_N(p_n)\gamma_5 u_N(p_2), \quad (26)$$

$$\mathcal{M}_{\Delta^*(1920)} = \frac{\sqrt{2} g_{\pi NN} g_{\Delta^*(1910)N\pi} g_{\Delta^*(1910)\Sigma K}}{m^2_{\Delta^*(1920)}} \times F_\pi^{NN}(q_\pi^2) F_\pi^{\Delta^* N}(q_\pi^2) F_{\Delta^*}(q_{\Delta^*}^2) \times \bar{u}_\Sigma(p_\Sigma)(p_K)_\mu G^{\mu\nu}_{\Delta^*}(q_{\Delta^*})(p_\pi)_\nu \times u_N(p_1) G_\pi(q_\pi) \bar{u}_N(p_n)\gamma_5 u_N(p_2), \quad (27)$$

where u_Σ and u_N are the dirac wave functions of the Σ baryon and the nucleon, respectively. The p_1 and p_2 denote the four-momentum of the initial protons. The above amplitudes are for the diagrams depicted in Fig. 1(a). For Fig. 1(b), we only need to exchange p_1 with p_2 in the above formula.

The influence of the $n\Sigma^+$ final state interaction (FSI) on the near-threshold behavior is possibly weaker than the $N\Lambda$ interaction as suggested in the literature [14,15,17]. This FSI effect, instead of the subthreshold $\Delta^*(1620)$, would give the near threshold enhancement in the total cross section. This gives rise to alternative solutions of solutions I and II. For the moment we do not have detailed information on this $n\Sigma^+$ FSI, so we do not know the magnitude of the impact of this FSI on the total cross section. For these reasons we simply factor the amplitudes as [40]

$$\mathcal{M}'_I = (\mathcal{M}_{\Delta^*(1620)} + \mathcal{M}_{\Delta^*(1910)} + \mathcal{M}_{\Delta^*(1920)}) T_{n\Sigma}, \quad (28)$$

$$\mathcal{M}'_{II} = (\mathcal{M}_{\Delta^*(1620)} + \mathcal{M}_{\Delta^*(1750)} + \mathcal{M}_{\Delta^*(1920)}) T_{n\Sigma}. \quad (29)$$

The $T_{n\Sigma}$ is the Jost function describing the $n\Sigma^+$ final state interaction and goes to unity if no FSI. In analogy to the $p\Lambda$ FSI in $pp \to pK^+\Lambda$ reaction [41], we take the same formula to depict the $T_{n\Sigma}$ as used in Ref. [23]:

$$T_{n\Sigma} = \frac{q + i\beta}{q - i\alpha},$$

where q is the internal momentum of the n-Σ^+ subsystem. Adjusting our numerical calculations to the experiment data and also referring the $p\Lambda$ interaction in the $pp \to pK^+\Lambda$ reaction [41], the values of the α and β are chose to be

$$\alpha = -70 \text{ MeV}, \quad \beta = 280 \text{ MeV}.$$

The scattering length and effective range can be calculated by α and β,

$$a = \frac{\alpha + \beta}{\alpha\beta}, \quad r = \frac{2}{\alpha + \beta}.$$

The above values of α and β correspond to the scattering length $a = 2.1$ fm and effective range $r = 1.9$ fm, which is close to the $a = 1.6$ fm and $r = 3.2$ fm in Ref. [23].

In our model, the initial state interaction (ISI) is not considered because it is difficult to treat the ISI unambiguously due to the lack of the accurate NN interaction model at such high incident beam energies. Hanhart and Nakayama [42] claim that the ISI has practically little influence on the energy dependence of the meson production cross section of nucleon-nucleon collisions close to threshold, and the reduction factor to the cross section can be roughly estimated by the NN phase shifts and inelasticities. In our paper, we do not consider this reduction factor because this estimation is rough so it would cause uncertainty in the model. In fact, the cut-off values in form factors partly play the role of this reduction factor, as prescribed in previous studies of nucleon-nucleon collisions [18–26]. This is possibly the reason that the used cut-off values are smaller than the usual ones.

The total cross section of the $pp \to nK^+\Sigma^+$ reaction could integrate the invariant amplitudes in the three-body phase space,

$$d\sigma(pp \to nK^+\Sigma^+) = \frac{m_p^2}{\sqrt{(p_1 \cdot p_2) - m_p^4}} \left(\frac{1}{4} \sum_{\text{spins}} |\mathcal{M}|^2 \right) \times (2\pi)^4 d\Phi_3(p_1 + p_2; p_n, p_K, p_\Sigma), \quad (30)$$

where the three-body phase space is defined as [39]

$$d\Phi_3 = 4 m_n m_\Sigma \delta^4 \left(p_1 + p_2 - \sum_{i=1}^{3} p_i \right) \prod_{i=1}^{3} \frac{d^3 p_i}{(2\pi)^3 2E_i}. \quad (31)$$

III. NUMERICAL RESULTS AND DISCUSSION

With the FOWL code in the CERN program library, the proton beam energy (T_p) dependence of the total cross sections for the $pp \to nK^+\Sigma^+$ reaction are calculated. As we have mentioned in Sec. II, we proposed two solutions to interpret the role and contribution of Δ^{*++} resonances in $pp \to nK^+\Sigma^+$ reaction. In this section, Figs. 4 and 5 present the numerical results of solution I and Fig. 6 and 7 are the calculations for solution II.

In solution I as shown in Fig. 4, it is found that the $\Delta^*(1910)$ resonance is dominant at high energy. The contributions of the

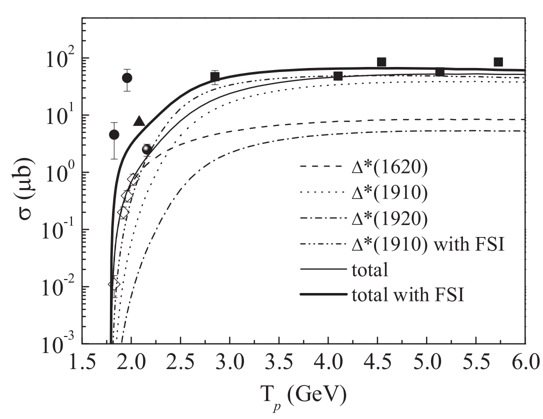

FIG. 4. The calculated total cross section versus T_p for the $pp \to nK^+\Sigma^+$ reaction in solution I compared to the data from old measurement (solid squares) [12], COSY-11 (solid circles) [13], COSY-ANKE (hollow diamonds and solid ball) [14,15,17], and HIRES (solid triangles) [16]. The dashed, dotted, and dash-dotted curves are contributions from the $\Delta^*(1620)$, $\Delta^*(1910)$, and $\Delta^*(1920)$, respectively. The dash-dot-dotted curve is the contribution of $\Delta^*(1910)$ with the $n\Sigma^+$ FSI. The solid and bold curves are the total contribution without and with the $n\Sigma^+$ FSI, respectively.

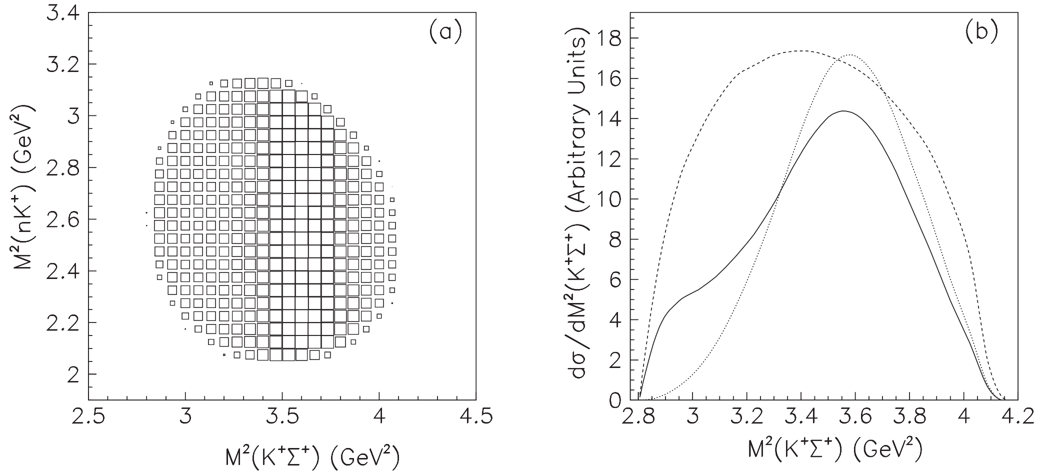

FIG. 5. The Dalitz plot (a) and invariant mass spectrum (b) for the $pp \to nK^+\Sigma^+$ reaction at beam energy $T_p =$ 2.8 GeV in solution I without FSI. The solid line is the total contribution of the $\Delta^*(1620)$, $\Delta^*(1910)$, and $\Delta^*(1920)$ resonances and the dotted line is that with $\Delta^*(1620)$ turned off. The dashed curve denote the pure phase space distribution.

$\Delta^*(1920)$ resonance are presented to be negligible, which is consistent with the results in Refs. [23,24]. In the very close-to-threshold energies, the contribution mainly comes from the $\Delta^*(1620)$ resonance. It is noted that the contribution from the $\Delta^*(1620)$ is not as large as the calculations in Refs. [23,24] and nearly one order smaller than that of the $\Delta^*(1910)$ at the beam energy $T_p > 2.5$ GeV, because we use smaller coupling constants of $\Delta^*(1620)K\Sigma$ and cut-off in the form factors. The total contribution from these three resonances [see the amplitude in Eq. (1)] are in good agreement with the COSY-ANKE data [12,14,15]. However, the role of the $\Delta^*(1620)$ could be replaced by the strong $n\Sigma^+$ FSI, see the dash-dot-dotted curve in Fig. 4. If the $\Delta^*(1620)$ and strong $n\Sigma^+$ FSI are both included in the model [see Eq. (28)], the HIRES data [16] could be fitted, as can bee seen by the bold curve in Fig. 4.

At the near threshold region, the Dalitz plot and invariant mass spectra are close to the distributions of pure phase space so they give us little information. The measurements at higher energies can give us more clues of contributing resonances. Since the kinetic energy of the proton beam T_p can reach up to about 2.8 GeV at COSY, we calculate the Dalitz plot and invariant mass spectra at $T_p =$ 2.8 GeV. Figure 5 depicts our model prediction of the Dalitz plot and invariant mass spectra in solution I of the amplitude without $n\Sigma^+$ FSI in Eq. (1). In Fig. 5(b), we notice that there is a bump for invariant mass spectra in the range of 2.8 GeV $^2 <$ $M^2(K^+\Sigma^+) <$ 3.2 GeV ^{2}, which comes from the contribution of the $\Delta^*(1620)$ resonance. So if invariant mass spectra could be measured with good precision, the role of the $\Delta^*(1620)$ resonance in the $K\Sigma$ production would be clarified.

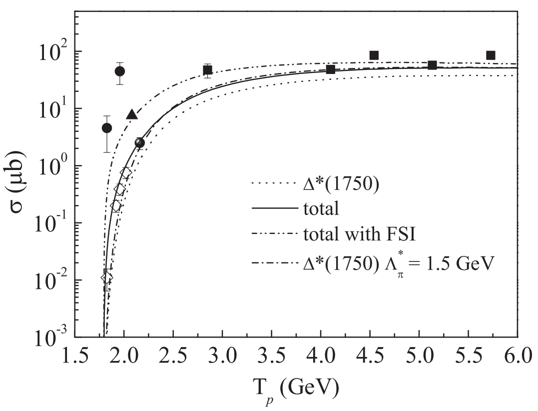

FIG. 6. The calculated total cross section versus T_p for the $pp \to nK^+\Sigma^+$ reaction in solution II. The data are the same as those in Fig. 4. The dotted and dash-dotted curves are the contribution from the $\Delta^*(1750)$ with $\Lambda^*_\pi = 1.0$ and 1.5, respectively. The dash-dot-dotted and solid curves are the total contribution with and without the $n\Sigma^+$ FSI, respectively.

In Fig. 6, we present the total cross sections for the $pp \to nK^+\Sigma^+$ reaction in our solution II. We find that the calculations with the amplitude in Eq. (2) can reproduce the COSY-ANKE data [12,14,15] quite well in the whole energy range. Here we use the same parameters for the $\Delta^*(1620)$ and $\Delta^*(1920)$ resonances as those in solution I. Similar to solution I, the $\Delta^*(1620)$ resonance is important in the very close-to-threshold energies and the contribution of $\Delta^*(1920)$ is small. The $\Delta^*(1750)$ takes the place in the $\Delta^*(1910)$ and dominates at high energies. As a result, it is seemed that either $\Delta^*(1910)$ or $\Delta^*(1750)$ can describe the data well and the total cross sections cannot resolve the mystery of mass position of the P_{31} resonance. Meanwhile, the total contribution with strong $n\Sigma^+$ FSI [see Eq. (29)] describe the HIRES data with good quality [16]. Moreover, it is worth noting that the contribution of $\Delta^*(1750)$ resonances alone with appropriate $\Lambda^*_\pi = 1.5$ GeV can describe the COSY-ANKE or HIRES data with or without strong $n\Sigma^+$ FSI, respectively, as shown in Fig. 6. This reflects the fact that the the role of subthreshold $\Delta^*(1620)$ resonance is very uncertain considering the present total cross section data if the dominant P_{31} state is $\Delta^*(1750)$. Fortunately, it would be studied in the invariant mass spectra, as pointed out above. Anyway, the HIRES data indicate strong $n\Sigma^+$ FSI in both solutions.

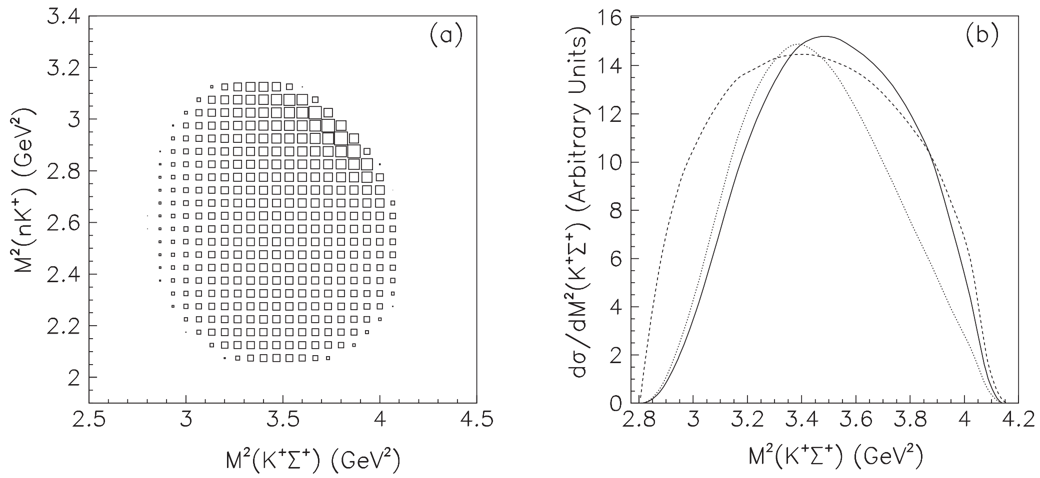

FIG. 7. The Dalitz plot (a) and the solid curve in invariant mass spectrum (b) for the $pp \to nK^+\Sigma^+$ reaction at beam energy $T_p = 2.8$ GeV with the contributions from the $\Delta^*(1750)$ resonance with FSI. The dotted curve is the $\Delta^*(1750)$ resonance without FSI, and the dashed curve denotes the pure phase space distributions.

In Fig. 7, we give the Dalitz plot and invariant mass spectra for the $pp \to nK^+\Sigma^+$ reaction at $T_p = 2.8$ GeV with the contribution of only the $\Delta^*(1750)$ resonance with $\Lambda^*_\pi = 1.5$. The influence of Λ^*_π on these observables is minor. Comparing with Fig. 5, we can see that the two schemes, the dominance of $\Delta^*(1910)$ or $\Delta^*(1750)$, are obviously distinguishable. So we expect that the new measurement of the invariant mass spectrum of the $pp \to nK^+\Sigma^+$ reaction at high energies could clarify the controversial spectrum of the Δ^* resonances. Meanwhile, the influence of the $n\Sigma^+$ FSI is mainly on the invariant mass spectra $M^2(n\Sigma^+)$ but the $\Delta^*(1620)$ resonance is more obvious in the $M^2(K^+\Sigma^+)$, so they can be discriminated in the Dalitz plot and invariant mass spectra as well.

IV. SUMMARY

The mass of the P_{31} state with isospin 3/2 is highly questionable at present. Though the $\Delta^*(1910)$ resonance is a four-star state in PDG [39] but it is missing in the dynamical coupled-channels analyses of the Excited Baryon Analysis Center (EBAC) at JLab [43], together with another four-star P_{33} state $\Delta^*(1920)$. In their updated analyses which include more channels, the $\Delta^*(1910)$ resonance appears [44,45]. The only P_{31} Δ^* state in the Giessen model [31–34] is the $\Delta^*(1750)$, and it is also seen in the old KSU analysis [46] and Pitt-ANL model [47]. The GWU analysis finds one P_{31} pole at $M = 1771$ MeV but assigned it as the $\Delta^*(1910)$ resonance due to its Breit-Wigner mass located at above 2.0 GeV [48]. The Jülich model finds a dynamical generated P_{31} state around 1750 MeV besides the genuine $\Delta^*(1910)$ resonance [25–28]. However, the $\Delta^*(1750)$ is only a one-star state in PDG [39]. The above situation shows that we still do not have enough knowledge of these Δ^* resonances. Our calculations in this paper would be helpful for understanding them better.

In this work, we have calculated the contributions from the $\Delta^*(1620)$, $\Delta^*(1750)$, $\Delta^*(1910)$, and $\Delta^*(1920)$ in the $pp \to nK^+\Sigma^+$ reaction and given two solutions to interpret the role and contribution of the Δ^{*++} resonances in this reaction based on the present data of total cross sections. In solution I, the contribution from the P_{31} $\Delta^*(1910)$ resonance is dominant at high energies. In solution II, we find that another P_{31} state $\Delta^*(1750)$ above threshold is most important, by combining with the experimental data of the $\pi^+p \to K^+\Sigma^+$ reaction. The present close-to-threshold data of total cross sections cannot pin down that the P_{31} state is $\Delta^*(1750)$ or $\Delta^*(1910)$. Only after the mass of the main resonance is determined, will the remaining free parameters, namely the decay ratios of resonances and cut-off in the form factors, be well determined by the measured data. Then the mechanism of $K\Sigma$ production would be explained with more confidence. At present, it is difficult to give a detailed error analysis of our model.

More seriously, the inconsistent close-to-threshold data from several groups result in the rather inconclusive status of the contribution at low energies. Either the subthreshold P_{31} $\Delta^*(1620)$ resonance or strong $n\Sigma^+$ FSI or both are possibly significant at the close-to-threshold region. If the HIRES data are only an upper bound of the total cross section as argued by Valdau and Wilkin [17], we can conclude that the $\Delta^*(1620)$ would be strongly coupled to the $K\Sigma$ if the $\Delta^*(1910)$ is responsible for the $K\Sigma$ production at high energies. However, if the strong coupling of the $\Delta^*(1750)$ to the $K\Sigma$ is confirmed, it is probable that the strong $n\Sigma^+$ interaction is excluded to some confidential level and the coupling of the $\Delta^*(1620)$ to the $K\Sigma$ has to be checked by the low range of $M^2(K^+\Sigma^+)$ in invariant mass spectra.

Fortunately, it is hoped that the invariant mass distributions and the Dalitz plot could discriminate these solutions because various contributions are evidently distinguishable as we have presented. Though the experiment would be challenging because of the neutron in the final states, it is encouraging to measure these observables in the future considering the very controversial location of the Δ^* resonance and their coupling to the $K\Sigma$ channel.

ACKNOWLEDGMENTS

X.Y.W. is grateful to Dr. Qing-Yong Lin for valuable discussions and help. This project is partly supported by the National Basic Research Program (973 Program Grant No. 2014CB845406) and the National Natural Science Foundation of China (Grant Nos. 11347156, 11405222, 11105126, and 11475227). We acknowledge the One Hundred Person Project of Chinese Academy of Sciences (Y101020BR0).

[1] S. Capstick and N. Isgur, Phys. Rev. D **34**, 2809 (1986).
[2] U. Löring, B. C. Metsch, and H. R. Petry, Eur. Phys. J. A **10**, 395 (2001).
[3] L. Ya. Glozman and D. O. Riska, Phys. Rep. **268**, 263 (1996).
[4] C. Helminen and D. O. Riska, Nucl. Phys. A **699**, 624 (2002).
[5] J. Bulava, R. G. Edwards, E. Engelson *et al.*, Phys. Rev. D **82**, 014507 (2010).
[6] R. G. Edwards, J. J. Dudek, D. G. Richards, and S. J. Wallace, Phys. Rev. D **84**, 074508 (2011).
[7] M. Dugger *et al.* (CLAS Collaboration), Phys. Rev. C **88**, 065203 (2013); **89**, 029901 (2014).
[8] M. Gottschall *et al.* (CBELSA/TAPS Collaboration), Phys. Rev. Lett. **112**, 012003 (2014).
[9] A. Lleres *et al.* (GRAAL Collaboration), Eur. Phys. J. A **39**, 149 (2009).
[10] G. Mandaglio *et al.* (Graal Collaboration), Phys. Rev. C **82**, 045209 (2010).
[11] R. Koniuk and N. Isgur, Phys. Rev. Lett. **44**, 845 (1980).
[12] A. Baldini, V. Flamino, W. G. Moorhead, and D. R. O. Morrison, in *Landolt – Börnstein, Numerical Data and Functional Relationships in Science and Technology*, Vol. 12, Total Cross Sections of High Energy Particles, edited by H. Schopper (Springer-Verlag, Berlin, 1988).
[13] T. Rożek *et al.*, Phys. Lett. B **643**, 251 (2006).
[14] Yu. Valdau *et al.*, Phys. Lett. B **652**, 245 (2007).
[15] Yu. Valdau *et al.*, Phys. Rev. C **81**, 045208 (2010).
[16] A. Budzanowski *et al.* (HIRES Collaboration), Phys. Lett. B **692**, 10 (2010).
[17] Yu. Valdau and C. Wilkin, Phys. Lett. B **696**, 23 (2011).
[18] K. Tsushima, S. W. Huang, and A. Faessler, Phys. Lett. B **337**, 245 (1994).
[19] K. Tsushima, A. Sibirtsev, and A. W. Thomas, Phys. Lett. B **411**, 9 (1997); **421**, 413 (1998).
[20] K. Tsushima, A. Sibirtsev, A. W. Thomas, and G. Q. Li, Phys. Rev. C **59**, 369 (1999); **61**, 029903 (2000).
[21] A. Sibirtsev, K. Tsushima, W. Cassing, and A. W. Thomas, Nucl. Phys. A **646**, 427 (1999).
[22] R. Shyam, Phys. Rev. C **73**, 035211 (2006).
[23] J. J. Xie and B. S. Zou, Phys. Lett. B **649**, 405 (2007).
[24] Xu Cao, Xi-Guo Lee, and Qing-Wu Wang, Chin. Phys. Lett. **25**, 888 (2008).
[25] A. M. Gasparian, J. Haidenbauer, C. Hanhart, L. Kondratyuk, and J. Speth, Phys. Lett. B **480**, 273 (2000).
[26] A. M. Gasparian, J. Haidenbauer, C. Hanhart, L. Kondratyuk, and J. Speth, Nucl. Phys. A **684**, 397 (2001).
[27] M. Döring, C. Hanhart, F. Huang *et al.*, Nucl. Phys. A **851**, 58 (2011).
[28] D. Rönchen, M. Döring, F. Huang *et al.*, Eur. Phys. J. A **49**, 44 (2013).
[29] A. V. Anisovich, E. Klempt, V. A. Nikonov *et al.*, Eur. Phys. J. A **47**, 27 (2011).
[30] A. V. Anisovich, R. Beck, E. Klempt *et al.*, Eur. Phys. J. A **48**, 15 (2012).
[31] G. Penner and U. Mosel, Phys. Rev. C **66**, 055211 (2002).
[32] G. Penner and U. Mosel, Phys. Rev. C **66**, 055212 (2002).
[33] V. Shklyar, G. Penner, and U. Mosel, Eur. Phys. J. A **21**, 445 (2004).
[34] Xu Cao, V. Shklyar, and H. Lenske, Phys. Rev. C **88**, 055204 (2013).
[35] W. H. Liang, P. N. Shen, J. X. Wang, and B. S. Zou, J. Phys. G **28**, 333 (2002).
[36] R. Brockmann and R. Machleidt, Phys. Rev. C **42**, 1965 (1990).
[37] Z. Lin, C. M. Ko, and B. Zhang, Phys. Rev. C **61**, 024904 (2000).
[38] V. Baru, C. Hanhart, M. Hoferichter, B. Kubis, A. Nogga, and D. R. Phillips, Nucl. Phys. A **872**, 69 (2011).
[39] K. A. Olive *et al.* (Particle Data Group), Chin. Phys. C **38**, 090001 (2014).
[40] M. L. Goldberger and K. M. Watson, *Collision Theory* (John Wiley and Sons, New York, 1976).
[41] A. Sibirtsev *et al.*, Eur. Phys. J. A **27**, 269 (2006); **29**, 363 (2006).
[42] C. Hanhart and K. Nakayama, Phys. Lett. B **454**, 176 (1999).
[43] N. Suzuki, B. Juliá-Díaz, H. Kamano, T.-S. H. Lee, A. Matsuyama, and T. Sato, Phys. Rev. Lett. **104**, 042302 (2010).
[44] H. Kamano, S. X. Nakamura, T.-S. H. Lee, and T. Sato, Phys. Rev. C **88**, 035209 (2013).
[45] H. Kamano, Phys. Rev. C **88**, 045203 (2013).
[46] D. M. Manley and E. M. Saleski, Phys. Rev. D **45**, 4002 (1992).
[47] T. P. Vrana, S. A. Dytman, and T. S. H. Lee, Phys. Rep. **328**, 181 (2000).
[48] R. A. Arndt, W. J. Briscoe, I. I. Strakovsky, and R. L. Workman, Phys. Rev. C **74**, 045205 (2006).